OPEN

Route to optimal generation of soft X-ray high harmonics with synthesized two-color laser pulses

Cheng Jin[1], Guoli Wang[1,2], Anh-Thu Le[1] & C. D. Lin[1]

[1]J. R. Macdonald Laboratory, Department of Physics, Kansas State University, Manhattan, Kansas 66506, USA, [2]College of Physics and Electronic Engineering, Northwest Normal University, Lanzhou 730070, P. R. China.

High harmonics extending to X-rays have been generated from gases by intense lasers. To establish these coherent broadband radiations as an all-purpose tabletop light source for general applications in science and technology, new methods are needed to overcome the present low conversion efficiencies. Here we show that the conversion efficiency may be drastically increased with an optimized two-color pulse. By employing an optimally synthesized 2-μm mid-infrared laser and a small amount of its third harmonic, we show that harmonic yields from sub- to few-keV energy can be increased typically by ten-fold over the optimized single-color one. By combining with favorable phase-matching and together with the emerging high-repetition MHz mid-infrared lasers, we anticipate efficiency of harmonic yields can be increased by four to five orders in the near future, thus paving the way for employing high harmonics as useful broadband tabletop light sources from the extreme ultraviolet to the X-rays, as well as providing new tools for interrogating ultrafast dynamics of matter at attosecond timescales.

I n science and technology, light sources in specific spectral regions are often needed for different applications. Some large national facilities have been built to provide powerful broadband tunable lights, for synchrotron radiations or free-electron X-ray lasers. On the other hand, for wide applications it is desirable that small tabletop light sources be available in individual laboratories. Today such broadband coherent lights have been generated as high-order harmonics in gases by intense femtosecond lasers, ranging from extreme ultraviolet (XUV) to soft X-rays, but their intensities are still too weak for most applications.

High-order harmonic generation (HHG) is an extremely nonlinear process in which ultrashort coherent lights are produced when atoms or molecules are exposed to an intense laser pulse. This is usually achieved with the conventional Ti:sapphire lasers operating at the wavelength of 0.8 μm[1]. In recent years advance of mid-infrared (MIR) lasers with wavelength of a few microns has made it possible to extend high harmonics to the soft X-ray region[2–4]. It is well-known that the cutoff photon energy by a laser with intensity I_L and wavelength λ_L is given by $\hbar\omega = I_p + 3.17U_p$, where the ponderomotive energy $U_p \sim I_L\lambda_L^2$, with I_p the ionization potential of the target and $\hbar$ the reduced Planck's constant. However, HHG yield from each atom has been shown[5–8] to drop roughly like $\lambda_L^{-(4-6)}$ and further reduction occurs if the propagation of harmonics in the gas medium is accounted for[9], resulting in very unfavorable scaling law for harmonics[10,11] as the laser wavelength is increased. Thus, in spite of keV harmonics have been generated with MIR driving lasers, the low conversion efficiency has prevented them from becoming useful light sources for many applications in the laboratories.

To increase harmonic yields, many efforts have been directed at creating favorable phase-matching conditions such that high harmonics are efficiently built up in the gas medium[12–14], or by temporal and spatial pulse shaping of the driving lasers[15,16]. An alternative approach is to synthesize multi-color sinusoidal fields to create waveforms that maximize harmonic emission from each atom. This approach has been explored often in the last two decades[17–27], usually by combining the 2nd or 3rd harmonic with the fundamental laser. More recently, advance in optical parametric amplification (OPA) and optical parametric chirped pulse amplification (OPCPA) technology[28,29] has made it possible to generate practically any optical waveforms by coherent wavelength multiplexing of ultra-broadband (over two or more octaves) pulses[30–38]. Despite these efforts, waveform synthesis has rarely been systematically investigated with the aim of achieving optimal harmonic yields[17,39]. In view of the increasing availability of MIR driving lasers[3,4,28] for generating sub-keV or keV harmonics, it is timely to investigate this optimization issue, particularly for harmonics near and above the water window, with the ultimate goal of generating useful tabletop coherent light sources.

Recently we proposed[39] a general scheme for optimizing a waveform with synthesized multi-color laser pulses that can enhance harmonic yield by one to two orders over the single-color one without the increase of the total laser power. In that work, we investigated how to optimize harmonic yields by adding one or two more color fields to a fixed mid-infrared laser. In the present work, we have another specific goal: we ask what are the best mid-infrared wavelength and target atom to use in order to generate the highest harmonic yields up to a given cutoff energy near the water window region or up to about 1 keV? Since our earlier work[39] has shown that an optimized two-color (fundamental and its third harmonic) waveform was already capable of generating nearly the same maximal harmonic yield as compared to the optimized three-color waveform, we restrict the simulation to two-color fields which would be easier to achieve in the laboratories than the multi-color ones[19]. As mentioned above harmonic cutoff is extended by increasing wavelength or laser intensity, but the harmonic yield drops very unfavorably with increasing wavelength. On the other hand, the increase of laser intensity may result in excessive ionization which reduces neutral atom density and excessive free electrons that are detrimental to good phase matching. These competing factors make the present simulations essential in order to identify optimal conditions for efficient harmonic generation in the sub- to few-keV region. Our simulations show that only a few percent of the third harmonic intensity of the fundamental is needed to achieve the enhancement reported here, thus they are doable with the present laser technology[19,37].

Methods

In a two-color field, we define the longer wavelength (λ_1) of the MIR laser as the fundamental and its third harmonic as the complementary one. As shown in Ref. 39 as well as in Supplementary Fig. S1, Supplementary Table S1 and Supplementary Note, the third harmonic is the best in a two-color synthesis. In the optimization we consider the synthesized waveform in one optical cycle of the fundamental given by

$$E(t) = E_1 \cos(\omega_1 t + \phi_1) + E_2 \cos(\omega_2 t + \phi_2). \quad (1)$$

Here E_i, ω_i, and ϕ_i (i=1, 2) are the respective amplitudes, angular frequencies and phases of the two pulses. The carrier-envelope phase (CEP) and the phase caused by the time-delay between the two pulses[31,34] are all included in ϕ_i. In the optimization, ϕ_1 is set to 0 for simplicity. We search parameters $\{\omega_1, E_1, E_2, \phi_2\}$ to maximize the single-atom HHG yield. Since optimization takes tens of thousands of iteration, and we are studying harmonics up to keV energies, an efficient algorithm of generating harmonics is desirable. Instead of the standard strong-field approximation (SFA)[40] used in our earlier paper[39], a simplified version of SFA[41,42] is used to calculate harmonics at each iteration. In this method the induced dipole is expressed as $D(t) = a(t) \exp[iS(t)]$ where

$$a(t) = g[t_b(t)]f[t_b(t)]\left[\frac{2\pi i}{\tau(t)}\right]^{3/2} g^*(t)d[v(t)]. \quad (2)$$

Here $g(t)$ is the ground-state amplitude, $t_b(t)$, $\tau(t)$ and $v(t)$ are the born time, excursion time, and velocity at time t for the returning electron. The transition dipole moment from the ground state to the continuum state is $d[v(t)]$. The action $S(t)$ is given as

$$S(t) = -\int_{t_b(t)}^{t}\left[\frac{v(t_b(t),t')^2}{2} + I_p\right]dt'. \quad (3)$$

The launched wave packet with zero transverse momentum component, $f(t)$, in Eq. (2), can be written as[42]

$$f(t) = -\frac{(2I_p)^{1/4}}{|E(t)|}\sqrt{\frac{\gamma(t)}{\pi}}, \quad (4)$$

where I_p is the ionization potential, $E(t)$ the laser's electric field, and $\gamma(t)$ the ionization rate.

We define the returning electron wave packet as

$$W'(t) = \frac{D(t)}{d[v(t)]}, \quad (5)$$

and assume that the ground state amplitude $g[t_b(t)] = g^*(t) = 1$. Note that Eq. (5) in the time domain is similar to the frequency-domain returning electron wave packet $W(\omega) = D(\omega)/d(\omega)$ used in the quantitative rescattering (QRS) model[43]. Only solutions that satisfy the classical recollision equations enter into Eq. (5).

For optimization we use the standard genetic algorithm (GA) by D. L. Carroll (FORTRAN genetic algorithm driver, version 1.7a, 2001, available at

http://cuaerospace.com/carroll/ga.html). We are interested in HHG over a broad energy region. In the tunnel ionization regime, ionization occurs in a very narrow time window, thus enhancement of one harmonic would automatically also enhance a broad range of harmonics. Since the optimization does not affect the recombination step in the harmonic generation, it is convenient to talk about returning electron wave packet (REWP)[44,45] that gives the optimal yield for the cutoff harmonic as the fitness function.

In addition to the fitness function, other constraints are imposed: (a) The cutoff energy should be more or less maintained at the pre-determined value. (b) The ionization level at the end of a single-cycle waveform should be less than a few percent. (c) In the plateau region, harmonics generated from "short"-trajectory electrons should be stronger than those from the "long" ones. These constraints are the same as in the previous work[39], but the parameter space $\{\omega_1, E_1, E_2, \phi_2\}$ (mentioned earlier) to be optimized is different. They are assumed not limited in the laboratory. We have checked that the present method of optimization agrees well with the one used in Ref. 39, but the calculation is much faster for harmonics up to keV's.

The constraints listed above are important since it marks the main difference between our approach from the work of Chipperfield et al.[17]. Constraint (b) is set to avoid excessive free electrons in the gas medium as they will cause phase-mismatch of harmonics and plasma defocusing of the laser beam. The ionization rate is calculated by the standard Ammosov-Delone-Krainov (ADK) formula[46,47]. Constraint (c) is imposed since only harmonics from "short"-trajectory electrons can be efficiently phase-matched in the gas medium. Constraint (a) is used since we are interested in maximal harmonic yields in a preset energy region, while Chipperfield et al.[17] was interested in the extension of harmonic cutoff energy. Our additional constraints incorporated effects of phase matching were absent in Ref. 17.

Once the waveform in one optical cycle of the fundamental is obtained, it is used to "stitch" a realistic synthesized two-color few-cycle pulse for a given pulse envelope. For simplicity, in our simulation below the pulse duration (full width at half maximum, or FWHM) for both colors are chosen to be three cycles of the fundamental. Each single-color laser is assumed to have Gaussian envelope and the time delay between them is set at zero. We then insert the dipole matrix element $d(\omega)$ to REWP in the context of the QRS model[43], to obtain laser-induced dipole $D(\omega)$ for each atom. The latter is then fed into three-dimensional (3-D) Maxwell's wave equation to simulate propagation of harmonics, where the co-propagation of the full driving laser beam is also included[9,48–51]. Since both the intensity and the geometric phase of a focused laser beam have spatial dependence, the optimized waveform is not maintained away from the center of the gas jet. Note that proper focusing conditions, such as beam waists and focusing positions, gas pressure, medium length, are all important factors that will determine the quality of phase-matching. Such optimization is better performed in the laboratory as numerical simulation would be too time-consuming.

Results

Figure 1 summarizes the main results of our simulations for cutoff energies from 0.2 to 1 keV. It shows the minimum (also the optimal) fundamental wavelength that can be used to generate maximal harmonic yields versus the desired cutoff energy for the three targets of Ar, Ne and He, respectively. While it is always possible to use longer wavelength to achieve the same cutoff energy, the harmonic yields reached would be weaker. The results are compared to the optimal
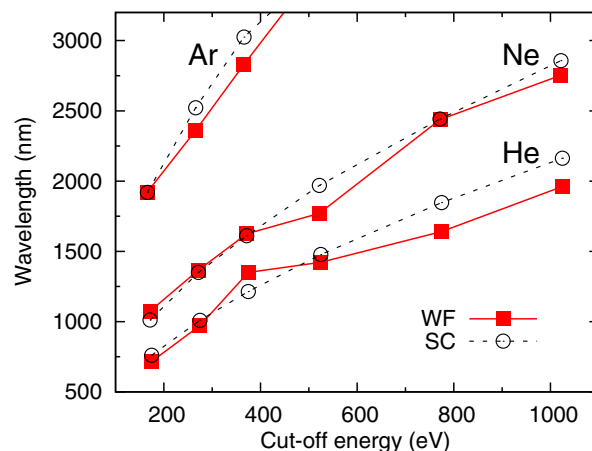

Figure 1 | Minimum fundamental wavelength for generating maximal harmonic yields versus the cutoff energy using Ar, Ne and He targets, for optimized waveform (WF) and single-color (SC) pulses. Waveform is synthesized by the fundamental laser and its 3rd harmonic. The ionization level in the simulation is set at 2% level. Other constraints in the optimization are discussed in the text.

single-color driving lasers. In both cases the degree of ionization is set at the same 2% level.

Note that single- and two-color optimized waveforms both have about the same minimum wavelength for a given cutoff energy, but the harmonic yields for the synthesized wave are much stronger (see below). This implies that harmonic cutoff energy is governed by the long-wavelength laser, but the third harmonic is needed to enhance the harmonic yield. This enhancement was explained in our early paper[39] as due to the strong increase of electric field during the time interval where "short"-trajectory electrons were ionized (see Fig. 1a of Ref. 39). The slope for Ar is the steepest because tunnel ionization rate depends on the ionization potential exponentially. The laser parameters for the optimized waveforms at different cutoff energies shown in the figure are given in the Tables 1–3. This figure clearly shows that by using 2-μm laser and its third harmonic, keV-photons can be produced using He as the generating gas.

We next consider how the results of Fig. 1 are derived. If one is to reach cutoff harmonics up to, say, 350 eV (the actual cutoff is 350 eV plus I_p of the target) which target and what fundamental wavelength are the best for reaching the highest yields? In Fig. 2(a) we compare single-atom HHG ($\propto \omega^4|D(\omega)|^2$) spectra of three targets calculated by the QRS model. The spectrum for Ne has the highest yields over a photon energy range of about 330 eV, followed by He and then by Ar. For the Ne target, the wavelengths of two lasers used are 1625 nm and its third harmonic, at a total intensity of 4.1×10^{14} W cm^{-2}. For the He target, the wavelengths are 1350 nm and its third harmonic, with total intensity of 6.2×10^{14} W cm^{-2} (for other parameters, see Tables 2 and 3). To generate harmonics up to a given cutoff energy with optimal yields, it is desirable to use the shortest fundamental wavelength due to unfavorable scaling of harmonic yields with increasing wavelength. However, a shorter fundamental wavelength has to be accompanied by a higher laser intensity in order to reach the desired cutoff energy. On the other hand, higher laser intensity cannot be running unrestrained since the total ionization yield is fixed at 2%. This can be controlled by choosing a target with higher binding energy, for atoms the highest one is helium. Still further complicated is the fact that harmonic yield also depends on photorecombination (or photoionization) cross section. The interplay of these factors would give the waveform as well as the favored target for generating maximal harmonic yields at a desired cutoff energy. The minimal fundamental wavelength for a given cutoff energy for each target shown in Fig. 1 was thus derived.

In Fig. 2(b) we compare the returning electron wave packets [defined as the modulus square of $W(\omega)$ in the QRS model] for the three targets where it shows that He is higher than Ne. However, as seen in Fig. 2(d), the photorecombination cross sections (PRCSs) for He are about ten times smaller than Ne, thus ending up that Ne target is more favorable for generating harmonics up to the 350 eV region.

The results of the propagated harmonics are shown in Fig. 2(c). In the simulation, the laser beam waist w_0 for each color in the waveform is fixed at 50 μm, the gas jet (1-mm long) is centered at $z_R/2$ after the focus where $z_R = \pi w_0^2/\lambda_1$ is the Rayleigh range of the fundamental laser. Thus for Ar, Ne and He, gas jet is at 1.4, 2.4 or 2.9 mm after the laser focus, respectively. Gas pressure with uniform distribution in the jet is 10 Torr. After propagation, the HHG spectrum from Ne is still the strongest. Note that the gas pressure used in the simulation is low. At higher pressure complications may result from phase mismatch and reshaping of the driving laser beam caused by the free electrons. When high gas pressure is used, absorption by the gas also becomes important. These additional target specific dependent properties make comparing harmonics from different targets complicated. In the absorption limited regime, helium would be the better gas for generating HHG for high-energy photons close to the keV region[13].

In Fig. 1 we show the minimum wavelength needed to reach a certain harmonic cutoff energy. Within the same photon energy region, can a longer wavelength (together with its third harmonic) generate more intense harmonics? In Fig. 3(a), we compare the macroscopic HHG spectra of Ne for three different cutoff energies. (Similar single-color results are shown in Supplementary Fig. S2, and single-atom HHG spectra of two-color waveforms are shown in Supplementary Fig. S3.) These spectra are generated by waveforms with fundamental wavelengths of 1075, 1367 and 1625 nm in order of increasing cutoff energy, respectively. Macroscopic conditions used to generate macroscopic HHG spectra are similar to Fig. 2. It is clear that the HHG yields drop rapidly when the harmonic cutoff energy is extended, or equivalently, when longer wavelength lasers are used. With the wavelength increases from 1075 nm to 1625 nm, i.e., by a factor of 1.5, the low-energy harmonics up to 150 eV drop by a factor of 125. Note that this result is based on the macroscopic conditions used in the simulation. If one is only interested in harmonics up to 150 eV with a longer wavelength laser, higher gas pressure can be used. For single-color laser an enhancement factor of 10 has been reported[11] if the pressure is optimized. Nevertheless, it is preferable to use the shortest wavelength laser to generate harmonics for each photon energy range as depicted in Fig. 1.

In Fig. 3 (b) we show a typical example of using He as a target for an optimized single-color wave and a two-color field, where the harmonic cutoff energy is over 500 eV and macroscopic propagation

Table 2 | Same as Table 1 but for Ne, I_p = 21.56 eV

Cutoff energy	WF				SC	
	λ_1	$|E_1|^2$	$|E_2|^2$	ϕ_2	λ_1	$|E_1|^2$
150 eV + I_p	1075	3.91	0.25	1.52π	1012	4.94
250 eV + I_p	1367	3.98	0.25	1.43π	1350	4.69
350 eV + I_p	1625	3.88	0.31	1.37π	1611	4.55
500 eV + I_p	1770	4.92	0.17	1.18π	1969	4.38
750 eV + I_p	2438	3.75	0.24	1.36π	2442	4.24
1000 eV + I_p	2753	3.94	0.21	1.31π	2857	4.14

Table 1 | Optimized laser parameters of waveform (WF) with varied cutoff energy. In the optimization, $\lambda_2 = \lambda_1/3$, ionization level is 2%, the phase of the fundamental wave is set to zero, i.e., $\phi_1 = 0$. Optimized laser parameters of single-color (SC) wave at the same ionization level are also shown. Laser wavelength (λ_1) is given in nm, peak intensities ($|E_1|^2$ and $|E_2|^2$) in 10^{14} W cm^{-2}. Cutoff energy is determined by the maximum returning electron energy (indicated in the table) plus ionization potential I_p. Target: Ar, I_p = 15.76 eV

Cutoff energy	WF				SC	
	λ_1	$|E_1|^2$	$|E_2|^2$	ϕ_2	λ_1	$|E_1|^2$
150 eV + I_p	1922	1.20	0.081	1.37π	1919	1.38
250 eV + I_p	2361	1.34	0.072	1.24π	2522	1.33
350 eV + I_p	2831	1.33	0.047	1.27π	3025	1.29

Table 3 | Same as Table 1 but for He, I_p = 24.59 eV

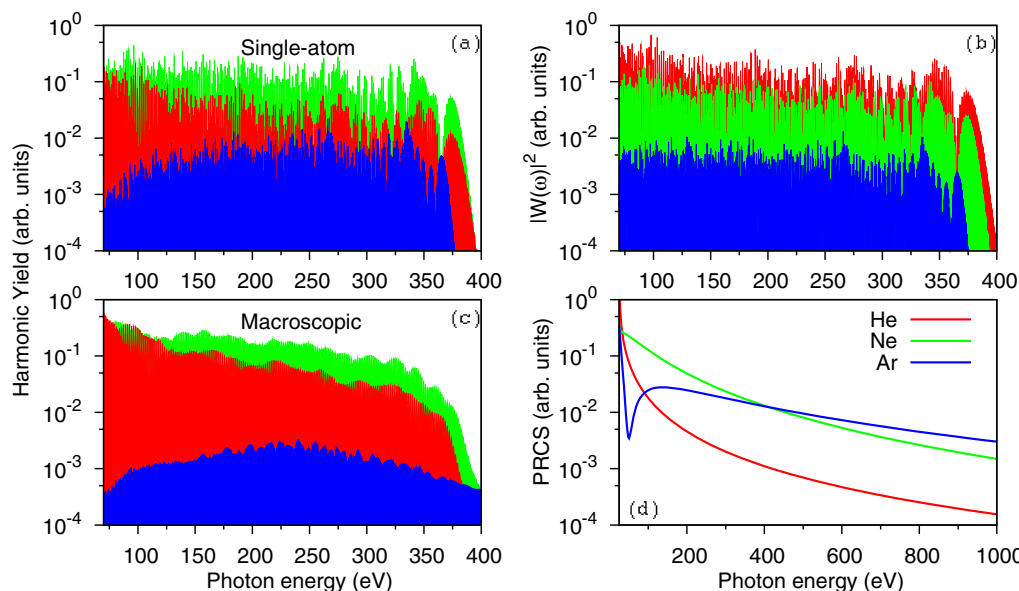| Cutoff energy	WF				SC	
	λ_1	$|E_1|^2$	$|E_2|^2$	ϕ_2	λ_1	$|E_1|^2$
150 eV + I_p	717	8.74	0.45	1.28π	761	8.75
250 eV + I_p	972	7.99	0.42	1.31π	1009	8.30
350 eV + I_p	1350	5.14	1.08	1.42π	1214	8.02
500 eV + I_p	1422	7.42	0.39	1.31π	1477	7.73
750 eV + I_p	1641	8.59	0.33	1.13π	1847	7.42
1000 eV + I_p	1961	7.86	0.39	1.19π	2163	7.22

Figure 2 | Comparison of maximal harmonic yields for optimized waveforms using three atomic targets. (a) Single-atom and (c) macroscopic HHG spectra calculated by using QRS model, and (b) returning electron wave packet calculated by SFA. The maximum returning electron energy is set at 350 eV. The fundamental wavelengths in the optimized waveforms are 2831, 1625 and 1350 nm for Ar, Ne and He, respectively. (d) Photorecombination cross sections (PRCSs) over a broad photon energy region are shown for the three targets.

effect has been included. The harmonic yields from the synthesized waveform show about one order increase in the plateau region to a few times stronger near the cutoff. According to Table 3, the intensity
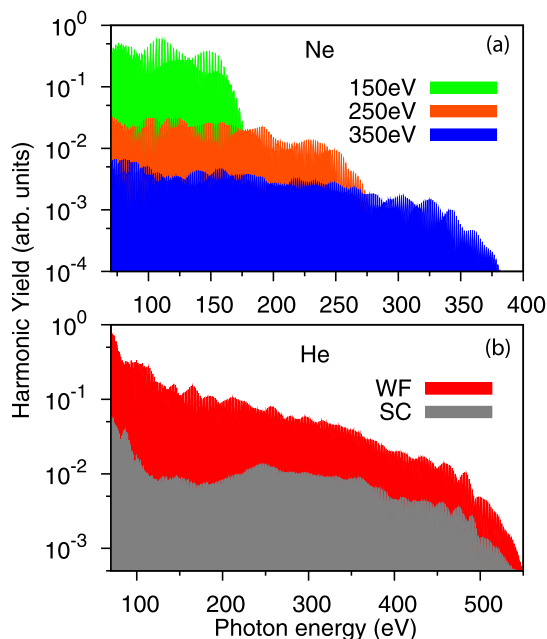

Figure 3 | Macroscopic spectra with two-color waveforms. (a) Macroscopic HHG spectra of Ne by using optimized waveforms to generate three different cutoff energies. The corresponding maximum returning electron energies are 150, 250 and 350 eV, using fundamental wavelengths of 1075, 1367 and 1625 nm, respectively. The total intensity is about 4.2×10^{14} W cm^{-2}, with the third harmonic about 10% of the intensity of the fundamental. Laser parameters are from Table 2. (b) Macroscopic HHG spectra generated from He with maximum returning electron energy of 500 eV, for the synthesized wave as compared to the single-color wave. The third harmonic intensity is about 5% of the fundamental wave which has wavelength of 1422 nm. The total peak intensity is about 7.8×10^{14} W cm^{-2}. Other laser parameters are given in Table 3.

of the third harmonic needed is only about 5% in order to achieve such an enhancement. The fundamental wavelength for the synthesized wave used is 1422 nm and 1477 nm for single-color wave. The peak intensity used is about 7.8×10^{14} W cm^{-2} for both waves. This result shows that a small amount of third harmonic can enhance HHG yield significantly for the long-wavelength laser because it is able to modify the driving waveform in such way that the contribution of "short" trajectories becomes dominant, while in the single-color field the contribution of "long" trajectories is dominant. (Single-atom HHG spectra are shown in Supplementary Fig. S3, and the corresponding time-frequency analysis is in Supplementary Fig. S4.) These arguments can be applied to other atoms and cutoff energies in Tables 1–3.

According to Fig. 1 the highest cutoff energy can be reached by 1600 nm and its third harmonic is about 400 eV with Ne as the target. We can optimize the peak field and phase of the two waves to achieve the highest yield at a given harmonic cutoff below 400 eV. In Fig. 4(a) we show the single-atom HHG for cutoff energies at 150, 200, 250 and 300 eV plus 21.56 eV, the I_p of Ne, respectively. The HHG yield for the 150 eV curve is the highest in the low-energy region, as compared to other curves where the cutoff energies are higher. All the four curves are generated with about the same total peak intensity. For the 150 eV curve, the peak intensity for the 1600 nm wave is half of the intensity of the 533 nm wave. In other words, the shorter 533 nm wavelength laser is the "fundamental" laser. For the 300 eV curve, the 533 nm wave is much weaker, with only 15% of the 1600 nm wave, i.e., the long wavelength 1600 nm one is the "fundamental" laser. The relative phase between the two waves remain about the same in all the four combinations; see laser parameters in Table 4. In conjunction with Fig. 3(a), we conclude that for the two-color fields, it is preferable to use the minimum wavelength from Fig. 1 to reach a given cutoff energy, and its third harmonic to enhance the harmonic yields.

Figure 4(b) displays the four optimized waveforms in one optical cycle of 1600 nm for the HHG shown in Fig. 4(a). The electric fields at the time of ionization (near -0.4 optical cycle in the figure) are essentially identical. On the other hand, the electric field near the return time for the "short"-trajectory electrons (near -0.1 optical cycle) starts to decrease its strength, less for the 300 eV curve and
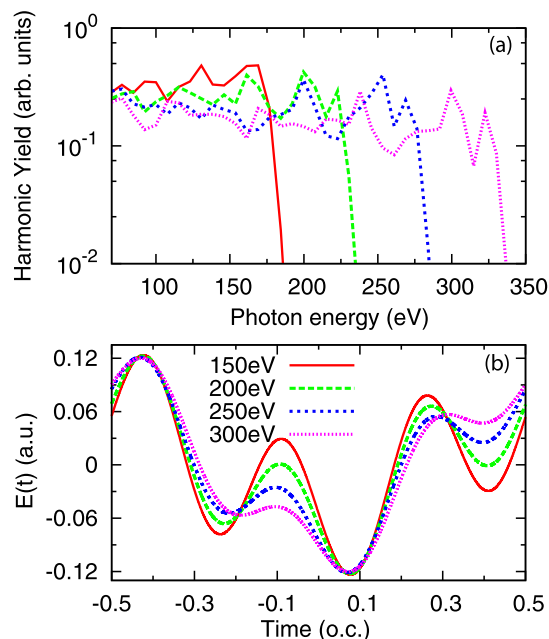
Figure 4 | Waveforms and HHG spectra with the fixed fundamental wavelength. (a) Single-atom HHG spectra of Ne with different cutoff energies by synthesizing 1600-nm laser and its 3rd harmonic. The spectra are smoothed by using the Bezier curve. The maximal returning electron energies are 150, 200, 250 and 300 eV. Laser parameters are from Table 4. (b) Optimized waveforms used to generate the harmonic spectra shown in (a). (o.c. stands for optical cycle of the 1600-nm laser.)

much more for the 150 eV one till its direction is reversed. Thus the kinetic energy gained by the electron between the born time and return time (best understood by the difference of vector potentials between the two instants, see Supplementary Fig. S5) is bigger for the 300 eV case and smaller for the 150 eV one, thus resulting in higher and lower cutoff energies, respectively.

Finally we note that the optimal relative phase between the fundamental and its 3rd harmonic fields is quite stable and in the range of 1.2π to 1.5π as shown in Tables 1–4 regardless of targets or cutoff energies. This is in agreement with both the experimental and theoretical results in Brizuela *et al.*[19]. They found that the relative phase of around 1 rad (equivalent to 1.32π if the carrier is assumed as a cosine function) led to the maximum HHG enhancement. To achieve the enhancement of a factor of 10 as predicted in this work, further optimization of the intensity of the third harmonics in the experiment is necessary. On the other hand, the precise control of CEP of each color and time delay between the two colors is also very crucial to realize the predictions in this work in experiments.

Discussion

In summary, we proposed a two-color synthesis scheme to achieve optimal harmonic yields ranging from the extreme ultraviolet to soft

Table 4 | Optimized laser parameters for waveforms with four different cutoff energies. In the optimization, $\lambda_1 = 1600$ nm, $\lambda_2 = \lambda_1/3$, and $\phi_1 = 0$. Peak intensities ($|E_1|^2$ and $|E_2|^2$) are in 10^{14} W cm^{-2}. Target: Ne, $I_p = 21.56$ eV

Cutoff energy	$|E_1|^2$	$|E_2|^2$	ϕ_2
150 eV + I_p	1.04	2.02	1.50π
200 eV + I_p	1.73	1.30	1.49π
250 eV + I_p	2.53	0.73	1.50π
300 eV + I_p	3.30	0.45	1.44π

X-rays. Between the two colors, one is the strong fundamental mid-infrared, the other is its weak third harmonic. For targets of argon, neon and helium, we optimized the shortest wavelength of the fundamental pulse that should be used for a given cutoff energy, as shown in Fig. 1. Our results also showed that optimized two-color field can always enhance the HHG yield by up to about ten times, when compared with the single-color one under the same generating condition, and requiring only about 5% intensity for the third harmonic which is reachable today. Indeed, some progress in waveform synthesis and optimization has been made[31,35–37]. Still much remains to be explored, including waveform control with multi-color lasers, or full phase control of a broadband supercontinuum over two octaves[52]. With the emergence of hundreds kHz and MHz MIR lasers on the horizon[53], the present simple two-color optimization, together with favorable phase matching conditions, make us to believe that high-order harmonics would soon be ready to become useful coherent tabletop light sources from the extreme ultraviolet to the X-rays. In the time domain, they also serve as intense attosecond pulses that can be used for attosecond-pump and attosecond-probe experiments for studying dynamics of electrons in matter in their intrinsic timescales.

1. Krausz, F. & Ivanov, M. Attosecond physics. *Rev. Mod. Phys.* **81**, 163–234 (2009).
2. Popmintchev, T. *et al.* Bright coherent ultrahigh harmonics in the keV X-ray regime from mid-infrared femtosecond lasers. *Science* **336**, 1287–1291 (2012).
3. Ishii, N. *et al.* Carrier-envelope phase-dependent high harmonic generation in the water window using few-cycle infrared pulses. *Nat. Commun.* **5**, 3331 (2014).
4. Hong, K.-H. *et al.* Multi-mJ, kHz, 2.1 μm optical parametric chirped-pulse amplifier and high-flux soft x-ray high-harmonic generation. *Opt. Lett.* **39**, 3145–3148 (2014).
5. Tate, J. *et al.* Scaling of wave-packet dynamics in an intense midinfrared field. *Phys. Rev. Lett.* **98**, 013901 (2007).
6. Schiessl, K., Ishikawa, K. L., Persson, E. & Burgdörfer, J. Quantum path interference in the wavelength dependence of high-harmonic generation. *Phys. Rev. Lett.* **99**, 253903 (2007).
7. Frolov, M. V., Manakov, N. L. & Starace, A. F. Wavelength scaling of high-harmonic yield: threshold phenomena and bound state symmetry dependence. *Phys. Rev. Lett.* **100**, 173001 (2008).
8. Le, A.-T., Wei, H., Jin, C., Tuoc, V. N., Morishita, T. & Lin, C. D. Universality of returning electron wave packet in high-order harmonic generation with midinfrared laser pulses. *Phys. Rev. Lett.* **113**, 033001 (2014).
9. Jin, C., Le, A. T. & Lin, C. D. Medium propagation effects in high-order harmonic generation of Ar and N_2. *Phys. Rev. A* **83**, 023411 (2011).
10. Shiner, A. D. *et al.* Wavelength scaling of high harmonic generation efficiency. *Phys. Rev. Lett.* **103**, 073902 (2009).
11. Colosimo, P. *et al.* Scaling strong-field interactions towards the classical limit. *Nature Phys.* **4**, 386–398 (2008).
12. Zhang, X. H. *et al.* Quasi-phase-matching and quantum-path control of high-harmonic generation using counterpropagating light. *Nature Phys.* **3**, 270–275 (2007).
13. Takahashi, E. J., Kanai, T., Ishikawa, K. L., Nabekawa, Y. & Midorikawa, K. Coherent water window X Ray by phase-matched high-order harmonic generation in neutral media. *Phys. Rev. Lett.* **101**, 253901 (2008).
14. Yakovlev, V. S., Ivanov, M. & Krausz, F. Enhanced phase-matching for generation of soft X-ray harmonics and attosecond pulses in atomic gases. *Opt. Express* **15**, 15351–15364 (2007).
15. Bartels, R. *et al.* Shaped-pulse optimization of coherent emission of high-harmonic soft X-rays. *Nature* **406**, 164–166 (2000).
16. Winterfeldt, C., Spielmann, C. & Gerber, G. Colloquium: Optimal control of high-harmonic generation. *Rev. Mod. Phys.* **80**, 117–140 (2008).
17. Chipperfield, L. E., Robinson, J. S., Tisch, J. W. G. & Marangos, J. P. Ideal waveform to generate the maximum possible electron recollision energy for any given oscillation period. *Phys. Rev. Lett.* **102**, 063003 (2009).
18. Watanabe, S., Kondo, K., Nabekawa, Y., Sagisaka, A. & Kobayashi, Y. Two-color phase control in tunneling ionization and harmonic generation by a strong laser field and its third harmonic. *Phys. Rev. Lett.* **73**, 2692–2695 (1994).
19. Brizuela, F. *et al.* Efficient high-order harmonic generation boosted by below-threshold harmonics. *Sci. Rep.* **3**, 1410 (2013).
20. Li, P.-C., Liu, I.-L. & Chu, S.-I. Optimization of three-color laser field for the generation of single ultrashort attosecond pulse. *Opt. Express* **19**, 23857–23866 (2011).
21. Kohler, M. C., Keitel, C. H. & Hatsagortsyan, K. Z. Attochirp-free high-order harmonic generation. *Opt. Express* **19**, 4411–4420 (2011).
22. Fieß, M. *et al.* Attosecond control of tunneling ionization and electron trajectories. *New J. Phys.* **13**, 033031 (2011).
23. Dudovich, N. *et al.* Measuring and controlling the birth of attosecond XUV pulses. *Nature Phys.* **2**, 781–786 (2006).

24. Shafir, D. *et al.* Resolving the time when an electron exits a tunnelling barrier. *Nature* **485**, 343–346 (2012).

25. Mauritsson, J. *et al.* Attosecond pulse trains generated using two color laser fields. *Phys. Rev. Lett.* **97**, 013001 (2006).

26. Kim, I. J. *et al.* Highly efficient high-harmonic generation in an orthogonally polarized two-color laser field. *Phys. Rev. Lett.* **94**, 243901 (2005).

27. Wei, P. *et al.* Selective enhancement of a single harmonic emission in a driving laser field with subcycle waveform control. *Phys. Rev. Lett.* **110**, 233903 (2013).

28. Schmidt, B. E. *et al.* Frequency domain optical parametric amplification. *Nat. Commun.* **5**, 3643 (2014).

29. Vaupel, A., Bodnar, N., Webb, B., Shah, L. & Richardson, M. Concepts, performance review, and prospects of table-top, few-cycle optical parametric chirped-pulse amplification. *Optical Engineering* **53**, 051507 (2014).

30. Vozzi, C. *et al.* Coherent continuum generation above 100 eV driven by an ir parametric source in a two-color scheme. *Phys. Rev. A* **79**, 033842 (2009).

31. Takahashi, E. J., Lan, P., Mücke, O. D., Nabekawa, Y. & Midorikawa, K. Attosecond nonlinear optics using gigawatt-scale isolated attosecond pulses. *Nat. Commun.* **4**, 2691 (2013).

32. Bandulet, H.-C. *et al.* Gating attosecond pulse train generation using multicolor laser fields. *Phys. Rev. A* **81**, 013803 (2010).

33. Siegel, T. *et al.* High harmonic emission from a superposition of multiple unrelated frequency fields. *Opt. Express* **18**, 6853–6862 (2010).

34. Takahashi, E. J., Lan, P., Mücke, O. D., Nabekawa, Y. & Midorikawa, K. Infrared two-color multicycle laser field synthesis for generating an intense attosecond pulse. *Phys. Rev. Lett.* **104**, 233901 (2010).

35. Huang, S.-W. *et al.* High-energy pulse synthesis with sub-cycle waveform control for strong-field physics. *Nature Photon.* **5**, 475–479 (2011).

36. Wirth, A. *et al.* Synthesized Light Transients. *Science* **334**, 195–200 (2011).

37. Haessler, S. *et al.* Optimization of quantum trajectories driven by strong-field waveforms. *Phys. Rev. X* **4**, 021028 (2014).

38. Ishii, N. *et al.* Quantum path selection in high-harmonic generation by a phase-locked two-color field. *Opt. Express* **16**, 20876–20883 (2008).

39. Jin, C., Wang, G., Wei, H., Le, A. T. & Lin, C. D. Waveforms for optimal sub-keV high-order harmonics with synthesized two- or three-colour laser fields. *Nat. Commun.* **5**, 4003 (2014).

40. Lewenstein, M., Balcou, P., Ivanov, M. Y., L'Huillier, A. & Corkum, P. B. Theory of high-harmonic generation by low-frequency laser fields. *Phys. Rev. A* **49**, 2117–2132 (1994).

41. Austin, D. R. & Biegert, J. Strong-field approximation for the wavelength scaling of high-harmonic generation. *Phys. Rev. A* **86**, 023813 (2012).

42. Gordon, A. & Kärtner, F. X. Quantitative Modeling of Single Atom High Harmonic Generation. *Phys. Rev. Lett.* **95**, 223901 (2005).

43. Le, A. T., Lucchese, R. R., Tonzani, S., Morishita, T. & Lin, C. D. Quantitative rescattering theory for high-order harmonic generation from molecules. *Phys. Rev. A* **80**, 013401 (2009).

44. Krause, J. L., Schafer, K. J. & Kulander, K. C. High-order harmonic generation from atoms and ions in the high intensity regime. *Phys. Rev. Lett.* **68**, 3535–3538 (1992).

45. Corkum, P. B. Plasma perspective on strong field multiphoton ionization. *Phys. Rev. Lett.* **71**, 1994–1997 (1993).

46. Ammosov, M. V., Delone, N. B. & Krainov, V. P. Tunnel ionization of complex atoms and of atomic ions in an alternating electromagnetic field. *Sov. Phys. - JETP* **64**, 1191–1194 (1986).

47. Tong, X. M. & Lin, C. D. Empirical formula for static field ionization rates of atoms and molecules by lasers in the barrier-suppression regime. *J. Phys. B* **38**, 2593–2600 (2005).

48. Gaarde, M. B., Tate, J. L. & Schafer, K. J. Macroscopic aspects of attosecond pulse generation. *J. Phys. B* **41**, 132001 (2008).

49. Tosa, V., Kim, H. T., Kim, I. J. & Nam, C. H. High-order harmonic generation by chirped and self-guided femtosecond laser pulses. I. Spatial and spectral analysis. *Phys. Rev. A* **71**, 063807 (2005).

50. Priori, E. *et al.* Nonadiabatic three-dimensional model of high-order harmonic generation in the few-optical-cycle regime. *Phys. Rev. A* **61**, 063801 (2000).

51. Brabec, T. & Krausz, F. Intense few-cycle laser fields: Frontiers of nonlinear optics. *Rev. Mod. Phys.* **72**, 545–591 (2000).

52. Chan, H. S. *et al.* Synthesis and measurement of ultrafast waveforms from five discrete optical harmonics. *Science* **331**, 1165–1168 (2011).

53. Krebs, M. *et al.* Towards isolated attosecond pulses at megahertz repetition rates. *Nature Photon.* **7**, 555–559 (2013).

Acknowledgments

Author contributions

C.J. and C.D.L. conceived the procedure of waveform optimization. C.J. performed all the calculations and analysis. G.W. and A.T.L. initiated the waveform optimization problem. A.T.L. provided the photoionization data. C.J. and C.D.L. wrote the manuscript. All authors discussed the results and reviewed the manuscript.

Additional information

Supplementary information accompanies this paper at http://www.nature.com/scientificreports

Competing financial interests: The authors declare no competing financial interests.

How to cite this article: Jin, C., Wang, G., Le, A.-T. & Lin, C.D. Route to optimal generation of soft X-ray high harmonics with synthesized two-color laser pulses. *Sci. Rep.* **4**, 7067; DOI:10.1038/srep07067 (2014).